Biochimica et Biophysica Acta 1858 (2016) 1955–1963

Contents lists available at ScienceDirect

Biochimica et Biophysica Acta

journal homepage: www.elsevier.com/locate/bbamem

On the dynamics of molecular self-assembly and the structural analysis of bilayer membranes using coarse-grained molecular dynamics simulations

Tanja Schindler [a,b], Dietmar Kröner [b], Martin O. Steinhauser [a,c,*]

[a] Fraunhofer–Institute for High–Speed Dynamics, Ernst–Mach–Institut, EMI, Eckerstrasse 4, 79104 Freiburg, Germany
[b] Albert–Ludwigs University of Freiburg, Department of Applied Mathematics, Hermann–Herder–Strasse 10, 79104 Freiburg, Germany
[c] Department of Chemistry, University of Basel, Klingelbergstrasse 80, CH-4056 Basel, Switzerland

ARTICLE INFO

Article history:
Received 21 December 2015
Received in revised form 27 March 2016
Accepted 17 May 2016
Available online 20 May 2016

Keywords:
Self-assembly
Molecular dynamics simulations
Bio-membranes
Coarse-graining
Structural properties
Phase diagram

ABSTRACT

We present a molecular dynamics simulation study of the self-assembly of coarse-grained lipid molecules from unbiased random initial configurations. Our lipid model is based on a well-tried CG polymer model with an additional potential that mimics the hydrophobic properties of lipid tails. We find that several stages of self-organization of lipid clusters are involved in the dynamics of bilayer formation and that the resulting equilibrium structures sensitively depend on the strength of hydrophobic interactions h_c of the lipid tails and on temperature T. The obtained stable lipid membranes are quantitatively analyzed with respect to their local structure and their degree of order. At equilibrium, we obtain self-stabilizing bilayer membrane structures that exhibit a bending stiffness κ_B and compression modulus K_C comparable to experimental measurements under physiological conditions. We present a phase diagram of our lipid model which covers a sol–gel transition, a liquid (or gel-like) phase including stable bilayer structures and vesicle formation, as well as a quasi–crystalline phase. We also determine the exact conditions for temperature T and degree of hydrophobicity h_c for stable bilayer formation including closed vesicles.

1. Introduction

Cell membranes are fascinating supramolecular aggregates that not only form a barrier between different compartments, or organelles, of cells but also harbor many chemical reactions essential to the existence and functioning of a cell [1]. For example, the plasma membrane serves as a barrier to prevent the contents of a cell from escaping and mixing with the surrounding medium. At the same time a cell's plasma membrane must enable the passage of critical nutrients into the cell and the passage of waste products out. Membranes must also be flexible to enable cells to change shape and they must have malleable topologies such that a cell can grow and divide into two separate parts, each of which has a completely closed contiguous membrane, a vesicle. Membranes in living biological systems have managed to balance these multiple demands by exploiting the special amphiphilic physical properties of the molecules that make them up.

The most common membrane constituents are lipid molecules with two physically separated subdomains, usually an elongated hydrophobic domain made up of fatty acid tails, associated with a hydrophilic head group [2]. The most abundant lipids in cell membranes are the phospholipids, molecules in which the hydrophilic head is linked to the rest of the lipid through a phosphate group [3]. The hydrophilic head groups of lipids dissolve readily in water because they contain polar groups that are easily incorporated in the hydrogen-bonding network of the surrounding water. In contrast, the hydrophobic hydrocarbon tails are uncharged and non-polar and thus try to aggregate in energetically and entropically favourable structures that minimize their contact with surrounding water molecules. Usually it is the correct mixture of asymmetric lipid molecules and proteins that tends to lead to the bilayer phase formation in aqueous environment. The nearly cylindrical shape of most membrane lipids makes the bilayer the most common geometrical organization for spontaneous self-assembly of lipid molecules in aqueous environment.

The fluid mosaic model of membranes by Singer and Nicolson [4] was of great heuristic value, and contributed to our general thinking about membrane organization by providing insights into the assembly of lipids into membranes resulting from diffusion processes. However, subsequent experimental evidence indicated that the lateral motion of membrane components was not free after all, but constraint by various molecular mechanisms, such as direct or indirect interactions with cytoskeleton elements. Many questions pertaining to cell membrane dynamics remain unanswered until today and many processes such as lateral segregation or transversal asymmetry are known to occur in membranes on vastly different spatiotemporal scales [5], [6]. For

* Corresponding author at: Fraunhofer Ernst-Mach Institute for High-Speed Dynamics (EMI), Eckerstrasse 4, 79104 Freiburg, Germany.
E-mail address: martin.steinhauser@emi.fraunhofer.de (M.O. Steinhauser).

http://dx.doi.org/10.1016/j.bbamem.2016.05.014
0005-2736/

example, membrane vesicle fusion in vivo has been reported to occur on a length scale of tens of nanometers and a timescale that is sub-millisecond, possibly faster than 100 microseconds [7], [8]. It is therefore not yet possible to visualize the re-formation of the lipids in a fusion pore experimentally. It is precisely at the spatial and temporal limits where instruments for direct observation fail that the membrane concept becomes fuzzy and unclear.

On the other hand, all-atom molecular dynamics (MD) simulations of lipid bilayers which resolve the dynamics of individual atoms are limited to extremely small membrane samples (tens of nanometers in extension) and traditionally fairly short time scales of at most a few hundred nanoseconds [9], [10]. With the ever growing speed of computers, today, simulations up to millisecond time scales are possible and even microsecond timescales are common on small computer clusters [11–14]. However, even with recent GPU-based simulations, it is still impossible to simulate bilayer structures or the formation of vesicles which are comparable in size to eukariotic cells [14–16], leaving coarse-grained (CG) simulations as the only currently available computational tool to access mesoscale phenomena, i.e. properties on a length scale of the order of several tens of microns.

CG models of macromolecules provide a route to explore biomolecular systems on larger length and time scales while still resolving important physical aspects of the lipid bilayer structure [17–25]. They constitute a class of mesoscale models, in which many atoms or groups of atoms are treated by fusing them together into new particles which act as individual interaction sites usually connected by entropic springs. Such models are becoming increasingly popular [26], [27] because they remain particle-based while greatly reducing the computational expense. Another advantage of CG methods is that the particle groups can be constructed at various resolutions, permitting the study of membranes at multiple scales. In the past few years, these developments even led to the emergence of a new research area where multiscale models are developed that couple the atomistic regime with a continuum description in an attempt to simulate whole cells with all major mechanical components, the cytoskeleton, the plasma membrane and the aqueous environment within the cytoplasm and outside the cell walls [28–31].

CG models were originally introduced in macromolecular modeling approaches for globular proteins in a 1976 pioneering paper by Warshel and Levitt [32]. Since then, CG models have found their way into polymer physics as so-called bead-spring models, taking advantage of universal scaling laws of long polymer chains due to their fractal nature [33–36], [37], as well as into geophysics, engineering and other areas of computational research [39], [40]. As reviewed by Saunders and Voth [41], CG models are nowadays routinely used in polymer- and biophysics for equilibrium [41–46] and non-equilibrium studies [47–49] of lipid bilayer membranes and provide a description of reduced complexity with respect to the molecular degrees of freedom [18], [50], [51]. Several past attempts have been made to obtain a stable, solvent-free, fluid phase bilayer in MD simulations. Some have even used analytical potentials with many-body (e.g. orientation-dependent or density dependent) terms [42], [44], [52]. More importantly, it has been shown that a stable fluid bilayer can be obtained using pairwise potentials alone [20], [53], [54].

In a CG description, sometimes also the solvent degrees of freedom are entirely removed. In such implicit solvent models, the solvent contributions to the interactions are treated through effective interaction terms such as stochastic forces, within an effective potential for the free energy [9], [44], [54–57]. For lipid molecules, the hydrophobic effects of the lipid tails due to the presence of solvent particles can be taken into account through the use of an attractive, smoothly tuneable interaction potential between the lipids. One example of such a tuneable potential was introduced by Steinhauser in computational polymer physics in the context of simulations of polymer melts and single polymers in solutions [36]. Usually, by adapting the CG approach, simulations gain at least three orders of computational efficiency. Such efficiency comes from a combination of factors. First, the size of the system reduces by at least 10-fold by using CG representation compared to atomistic structure. This size reduction increases computational efficiency around 10 times. Second, due to usually wider potential wells, CG simulations allow the use of much larger timesteps (100–500 fs) compared to 10 to 40 fs used in purely atomistic simulations. Together, these factors make CG simulations highly efficient compared to their atomistic counterpart [38]. Hence, by using this simplified modeling of polymer-solvent interactions results in a computational speed-up, making simulations of large-scale membrane structures possible.

In this paper we present an implicit-solvent molecular dynamics study of the clustering of lipid molecules, which start from unbiased random initial configurations and which finally form stable bilayer membranes or closed vesicles. In particular, in contrast to previous studies that included aspects of the dynamics of self-assembly [14], [44], [58–60], we investigate the successive steps in membrane formation during self-assembly with respect to energy minimization and the degree of order that is introduced in the system. We show that during self-assembly, the membrane undergoes several stages of clustering that minimize the free energy of the system, and finally lead to a stable, fluid, or gel-like bilayer structure where the lipid molecules exhibit strong fluctuations. The different stages of clustering can be monitored by the total potential energy of the system. In our analysis we find that the order parameter S_2 which we use to characterize the degree of order present in the systems, is indicative of major reorientations of the lipids during the process of self-assembly. In addition, results for the pair correlation functions and for the orientational order parameter for a whole range of different temperatures and varying levels of hydrophobicity of the lipid tails are presented. For our systems at equilibrium we further show that the bilayer structures exhibit a bending stiffness κ_B and a compression modulus K_C comparable to experimental measurements under physiological conditions. As for κ_B and K_C, the findings show that our systems represent realistic physiological conditions to a larger degree than in previous numerical studies of membrane bilayers and vesicles [58], [60–62]. We also analyze the exact conditions for temperature T and lipid interaction strength to obtain stable fluid bilayer phases including quasi-crystalline structures and closed vesicles. Such an analysis was not provided in previous numerical studies that included a phase diagram of bilayer membranes based on CG model parameters [52], [61].

2. Coarse-grained system and simulation method

We perform constant temperature molecular dynamics simulations using the MD simulation software package MD-CUBE which was originally developed by Steinhauser [36], [38] for coarse-grained (CG) macromolecular simulations of single polymers and melts of almost arbitrarily branched monomer connectivity. For studying lipid bilayer membranes, many different CG implicit-solvent models based on either MD [42], [57], [62–66] or Monte Carlo (MC) procedures [9], [52–55], [58], [67], [68] have been developed, each one capturing molecular details at different levels of resolution.

Our approach to coarse-graining lipids is based on a standard CG polymer model, Eqs. (1) to (3), that has been used in several studies of polymers [22], [38], [40]. In order to model the particular hydrophobic effect of lipids, we use an additional potential in Eq. (4), akin to one, that was introduced originally by Steinhauser to account for the effects of different solvent qualities in polymer solutions [36]. A similar model was also used for the simulation of a three–bead model of lipids where the lipid-lipid interaction is only effective between the first and last bead of the lipid [64]. Our model however is not limited to only three particles as it takes into account the interaction between all consecutive particles in the lipid, thus leading to smaller fluctuations at equilibrium. Our model is illustrated schematically in Fig. 1: In a first coarse-graining step, the hydrophobic and hydrophilic parts of the lipid are replaced

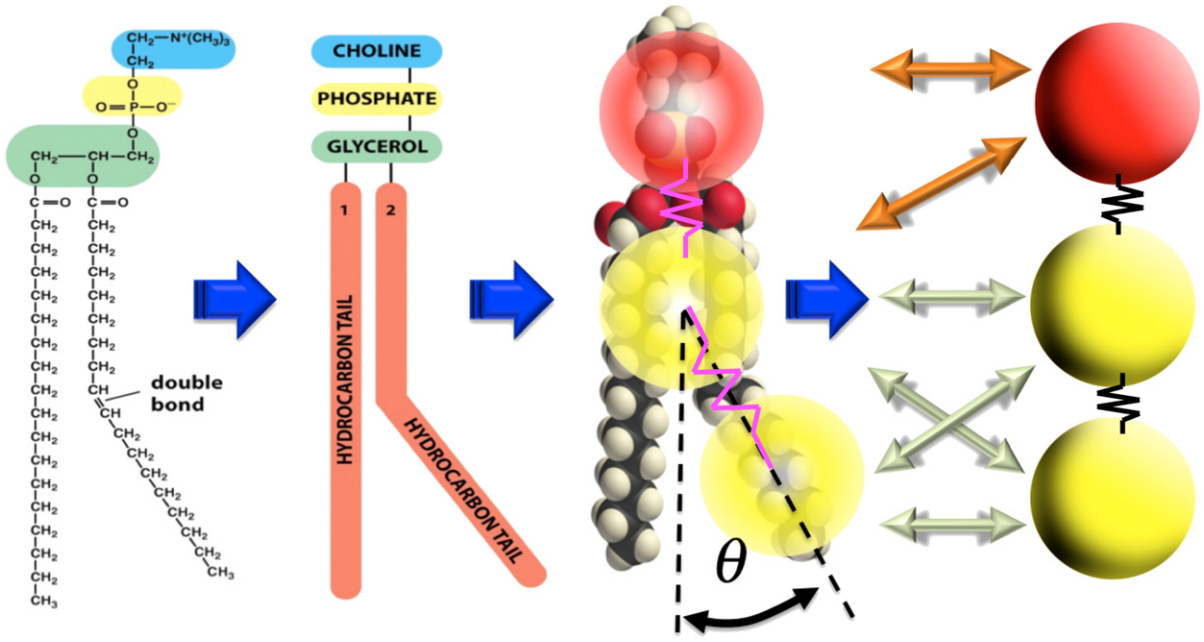

Fig. 1. Schematic of our CG model of lipid molecules: The most common structure of lipid molecules found in bio-membranes of eukaryotic cells, Phosphatidylcholine ($C_{40}H_{80}NO_8P$), as a formula and a space filling model which in essence is built from 5 parts: The hydrophilic head, choline is linked via a phosphate to glycerol, which in turn is linked to two hydrocarbon chains, forming the hydrophobic tail.

with a polymer model based on particles: Two particles are used for the tails, indicated in light-colored (yellow) spheres and one for the head, indicated in dark color (red). We note here, that the use of three particles is arbitrary and was done for reasons of simplicity – our model is by no means restricted to a certain number of CG particles in the polymer chain that substitutes the components of the lipid molecule. In a second step, the particles of our lipid model are connected using anisotropic springs according to Eq. (1). The standard excluded volume LJ interaction according to Eq. (2) between all beads is indicated in dark color (orange), and the angle θ for the bending potential of Eq. (3) is also drawn. Finally, the attractive potential of Eq. (4) between tail particles of different chains that mimics the hydrophobic interaction of the lipid tails with the aqueous environment is indicated with light–colored arrows (light-green).

The complex molecular structure is simplified by replacing the lipid structure with three spherical soft particles connected by elastic springs. The first particle which is color–coded in dark color (red) in Fig. 1, represents the hydrophilic head and the other two (in yellow color) the hydrophobic tails. We note here, that our model is in principle not restricted with respect to the number of particles per lipid, but we use a three-particle version of it here to ease the discussion of our results in light of the findings obtained in previous MD studies of membranes using CG models. Hence, Eqs. (1) to (4) model the structural and amphiphilic properties of the lipids. The mass points of a lipid chain are connected by anharmonic bonds with the potential

$$\Phi_{\text{bond}}(r) = \begin{cases} -\frac{1}{2}\alpha\, r_\infty^2 \ln\left[1-\left(\frac{r}{r_\infty}\right)^2\right] & \text{for} \quad r < r_\infty, \\ \infty & \text{for} \quad r \geq r_\infty, \end{cases} \tag{1}$$

where α is the force constant, r denotes the distance between two mass points, and r_∞ denotes the maximum bond length which we set to $r_\infty = 1.5\sigma$ in dimensionless (simulation) units. All other model parameters are also expressed in terms of simulation units given by ε and σ.

The finite size of a monomer of the lipid molecule is taken into account by the truncated Lennard-Jones (LJ) potential

$$\Phi_{\text{LJ}}(r) = \begin{cases} 4\varepsilon\left[\left(\frac{\sigma}{r}\right)^{12} - \left(\frac{\sigma}{r}\right)^{6}\right] + \varepsilon & \text{for} \quad r < r_{\text{cut}}, \\ 0 & \text{for} \quad r \geq r_{\text{cut}}, \end{cases} \tag{2}$$

In our simulations we set the cut-off radius to $r_{\text{cut}} = \sqrt[6]{2}\sigma$.

To straighten the lipids, a bending potential for all bonds depending on the bond angle θ (see Fig. 1) is used in the form

$$\Phi_{\text{bend}}(\theta) = \lambda(1 - \cos\theta), \tag{3}$$

where λ determines the stiffness of the lipid molecule.

The typical structures of self-assembling lipids arise from the hydrophobic and hydrophilic interactions of the lipid tails and heads, respectively, with the surrounding water molecules. When using a solvent-free model, the hydrophobic interactions of lipid tails with water can be modelled using an attractive potential between all tail particles of different lipid chains as indicated in Fig. 1 by the light–colored arrows:

$$\Phi_{\text{attr}}(r) = \begin{cases} -\xi & \text{for} \quad r < r_{\text{cut}}, \\ -\xi\cos^2\left(\frac{\pi(r - r_{\text{cut}})}{2h_c}\right) & \text{for} \quad r_{\text{cut}} \leq r \leq r_{\text{cut}} + h_c, \\ 0 & \text{else} \quad , \end{cases} \tag{4}$$

where h_c determines the range of the attractive potential, i.e. the larger h_c the greater the hydrophobicity of the lipid tails, ξ is a force constant, and r_{cut} is the same cutoff as in Eq. (2). A tuneable potential of this type (involving a cosine function) was introduced by Steinhauser [36] for the realistic MD simulation of polymer-solvent interactions with varying solvent qualities. A similar form of the potential of Ref. [36] which we use in Eq. (4) was later used in implicit solvent MD simulations of lipids (i.e. very short polymer chains) by Cooke et al. [64].

The interaction of all particles with the solvent is taken into account by a stochastic force $\vec{\Gamma}_i$ and a friction force, with a damping constant γ,

acting on each mass point m_i. All mass points m_i of the hydrophilic and hydrophobic part of the lipids are assumed to have the same mass m. The equations of motion of the system are then given by the Langevin equations

$$m\ddot{\vec{r}}_i = \vec{F}_i - \gamma m \dot{\vec{r}}_i + \vec{\Gamma}_i. \quad (5)$$

The force $\vec{F}_i$ is given by

$$\vec{F}_i = -\vec{\nabla}_{\vec{r}_i} \Phi_{\text{total}}, \quad (6)$$

and is the force due to the sum of the potentials in Eqs. (1)–(4). The stochastic force $\vec{\Gamma}_i$ is assumed to be stationary, random, and Gaussian (white noise). This ensures proper equilibration of the dilute initial system [22]. Also, for generating the equilibrium structures, we have implemented a Berendsen constant pressure bath according to Ref. [70].

2.1. Initial setup of coarse-grained lipid molecules

At the beginning of the simulation, the lipid chains are generated as follows: the center position of the first particle *i* of a chain is chosen randomly inside the simulation box. The position of the second particle is chosen in a random direction of the first one, at distance $r_{i,i+1} = 0.97\ \sigma$. The center position of the third particle of a lipid chain is chosen in the same way as the second but with the constraint that the distance to the first particle is $r_{i,i+2} = 1.02\ \sigma$. This is done to prevent the third particle from getting too close to the first one, which would immediately lead to strong repulsive LJ forces inside the chain and subsequent instability of the integration algorithm.

However, this procedure does not prevent particles of *different* chains from initially overlapping each other. Therefore, before starting the actual simulation run with the potentials given in Eqs. (1)–(4), we carry out a warm-up procedure, which integrates the system by gradually increasing the effect of the LJ potential as follows: First, the minimum distance $r_{\min}$ between all particles is calculated. Then, instead of calculating the LJ interactions between particles of different chains with the actual distance r in step n, a shifted distance of $r' = r + \Delta r - n/n_{\text{warmup}} \times \Delta r$ with $\Delta r = r_c - r_{\min}$ and $n \in \{1, \ldots, n_{\text{warmup}}\}$ is used. Thus, the full LJ potential is effective only after $n = n_{\text{warmup}}$ steps, which then allows for a fully stable integration of the equations of motion in Eq. (5). A more detailed description of our warm-up procedure can be found in Ref. [69].

3. Results and discussion

In this section we discuss the dynamics of the formation and equilibration of bilayer membrane structures based on energy minimization and an order parameter $S_2(\tau)$ derived from the second order Legendre polynomial. In our structural analysis we show that our obtained self-stabilizing equilibrium structures of bilayer membranes exhibit a bending stiffness κ_B and compression modulus K_C which are within the range of experimental measurements under physiological conditions. Finally, we present a phase diagram of our lipid model which includes a sol-gel transition, quasi-liquid and quasi-crystalline phase behavior and – in contrast to other CG studies that included a phase diagram [52], [61] – we also discuss the precise conditions for temperature T and hydrophobicity h_c for stable bilayer and closed vesicle formation.

3.1. Dynamics of lipid bilayer assembly and equilibration

Figure 2 shows the typical time evolution of membrane formation for a system with $N = 1000$ lipids, temperature $T = 1.0$, timestep $\Delta t = 0.01\tau$, where τ is the time unit of the simulation, $\alpha = 30\varepsilon/\sigma^2$, $r_\infty = 1.5\sigma$, $\kappa_B = 10\varepsilon/\sigma^2$ and $h_c = 1.5\sigma$. The snapshots are taken at simulation

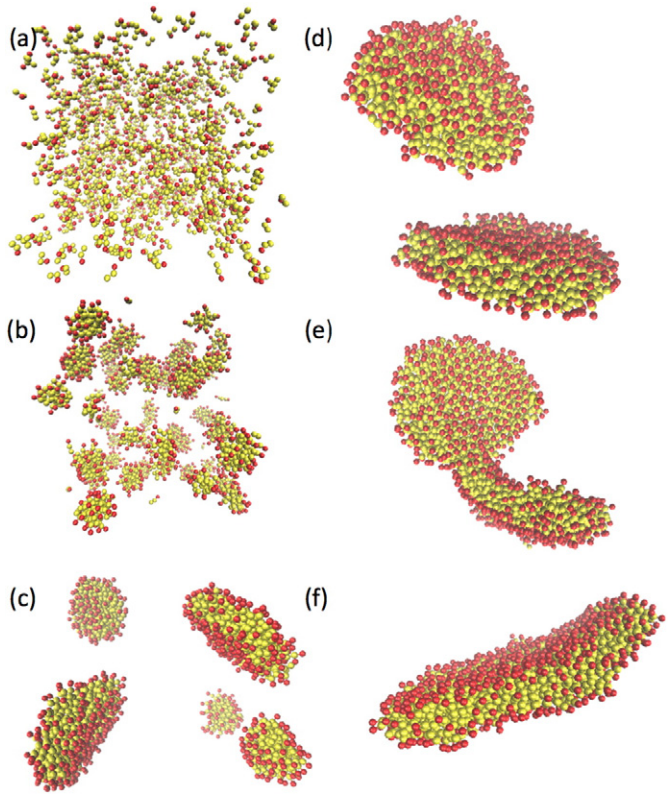

Fig. 2. Dynamics of bilayer membrane formation. The letters (a)–(f) correspond to points in time as described in the main text.

times (a) $\tau = 0$, (b) $\tau = 100$, (c) $\tau = 4000$, (d) $\tau = 18000$, (e) $\tau = 20200$, (f) $\tau = 22400$.

The start time $\tau = 0$ denotes the beginning of the actual integration after the warm-up procedure. As can be seen in Fig. 2, starting from a random distribution of lipid molecules, very quickly the lipids assemble to small clusters, which gradually merge into bigger clusters, while minimizing the number of hydrophobic tail particles on the surface of these clusters. Finally, due to our particular choice of parameters, and because we run the systems longer than in previous coarse-grained MD studies [58–60], [63], in the simulations presented in Fig. 2, one single bilayer membrane in fluid phase is formed. The snapshots presented in Fig. 2 (b) and particularly in (e) show one characteristic feature during lipid assembly, namely the occurrence of "lipid bridges" during merging of different membranes, which looks as though one membrane is "swallowed" by the other. This is consistent with one of the intermediate structures reported in recent all-atom MC simulations [14].

The time scale for occurrence of different stages in the self-assembly processes presented in Fig. 2 (very rapid initial clustering to form several smaller membranes, then gradual fusing) is consistent with what was reported in a relatively recent CG MD simulation study conducted by Noguchi [60] (Fig. 3 therein), but in contrast to that study which ends with 4 disjunct clusters, we present the dynamics until only one single equilibrated membrane remains. We note here, that the potential used in the study of Ref. [60] (a particle-based CG model of lipids) included orientation and angle-dependent functions of much more complexity and with more free fit-parameters compared to our CG model.

Many other studies dealing with membrane assembly were based on MC rather than MD methods [9], [52], [53], [67], [68]. In this case, there is no real timescale involved with the consecutive snapshots at different numbers of MC steps. Hence, these MC studies could best be compared with our investigations in terms of the *final* MC equilibrium

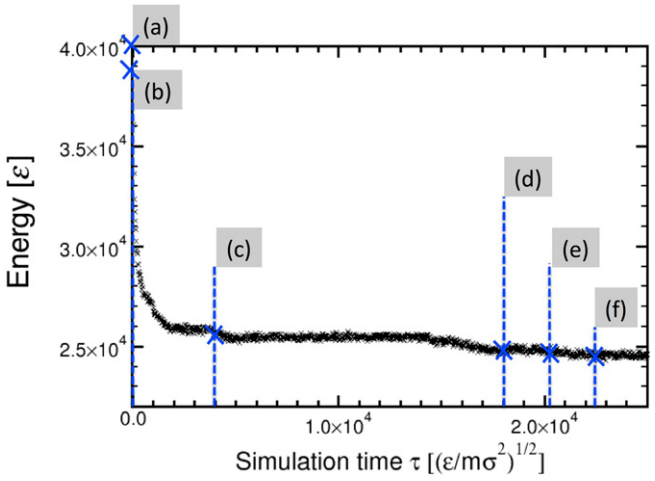

Fig. 3. Potential energy vs. simulation time τ. The letters (a)–(f) indicate different simulation times that correspond to the snapshots in Fig. 2.

structures. However, the very few snapshots of final configurations in these computational studies are not suitable for direct comparison with our snapshots provided in Fig. 2. For example, in Ref. [67], a two-tail coarse-grained MC model was used including 13 particles per lipid and all model parameters were fitted specifically to DPMC and DHPC. Because the snapshots were based on MC moves, no timescale was associated with them in the first place. In contrast to this, our model is a generic model where parameters have not been fitted to map a particular lipid molecule. In another publication by the same authors of the same year [68], they presented the same model along with two snapshots (initial state and final state) in comparably low quality with no further quantitative analysis. So, their final particle configuration (presumably at equilibrium) cannot soundly be compared with our quantitative findings. The major differences between the model used in Ref [68] and our model may account for the hexagonal, irregular structures which were reported in Ref. [68] and which we don't see at all in our final membrane structures.

In another MC study, Brannigan et al. [52] presented a MC-based model of cylindrical objects representing lipids and their assembly due to a relatively complex interaction model. In Ref. [53] they introduced a different, particle-based MC model with potentials taken from a publication of Goetz et al. [43] but the presented snapshots in both publications do not allow a well-founded comparison with our findings – they are not further quantitatively analyzed and not connected to structural properties in the way like we present our data of the self-organization dynamics in the following sections.

3.1.1. Energies and equilibration

The progress in self–assembly of lipid molecules can be tracked by monitoring the total potential energy of the system. When small lipid clusters merge into bigger clusters, the total surface area is decreased, thus reducing the free energy of the clustered system. While the system is approaching equilibrium, one can distinguish different energy levels in a plot of potential energy vs. time as displayed in Fig 3. Here, we display the potential energy curve for $\tau \in [0,\ 2.5\times10^4]$. The letters (a)–(f) in the figure indicate the different simulation times which correspond to the simulation snapshots in Fig. 2. The potential energy finally oscillates about a constant value, once the system has reached a stationary equilibrium state. We have checked this behavior in long simulation runs until a simulation time $\tau = 5\times10^5$.

3.1.2. Order parameter

To characterize the degree of structural order in the system of lipid molecules during self-assembly, we introduce an order parameter $S_2(\tau)$ based on the second order Legendre polynomial $P_2(\cos\vartheta)$:

$$S_2(\tau) = \langle P_2(\cos\vartheta(\tau))\rangle = \left\langle \frac{3}{2}\cos^2\vartheta(\tau) - \frac{1}{2}\right\rangle. \quad (7)$$

Here, $\vartheta(\tau)$ denotes the momentary deviation of the lipid direction vectors from the average normal vector of the membrane plane. This vector is estimated by calculating the average center of mass of all lipids located at the four edges of the membrane, separately for both sides of the bilayer. The connecting vector of these two centers of mass is our estimate for the normal membrane vector. Finally the lipid direction vector is defined as the vector connecting the center of mass of a head particle with the center of mass of the second tail particle. The values of the order parameter are in the range of $S_2(\tau)\in[-0.5,\ 1.0]$. For $S_2(\tau) = -0.5$, the average normal vector equals 0, and $S_2(\tau) = 0.0$ when the system does not show any order. Finally, $S_2(\tau) = 1.0$ corresponds to a perfect parallel alignment of the lipids. Typical liquid crystals exhibit values between $S_2(\tau) = 0.3$ and $S_2(\tau) = 0.8$.

Figure 4 exhibits how the system in Fig. 2, starting from a completely disordered, random initial state with $S_2(0) = 0.0$, slowly develops into an ordered, stationary state with values of $S_2(\tau)$ saturating just below $S_2 \approx 0.6$, which is within the typical range of liquid crystals for a fluid phase. Thus, our model membranes exhibit fluid-like behavior. The undulations of the values of $S_2(\tau)$ in Fig.4 are due to this fluidity of the membranes. The values of $S_2(\tau)$ at (a) and (b) are still practically 0, then at (c) we can see in Fig. 4 that the order of the system has increased considerably ($S_2(\tau) \approx 0.3$), due to merging of several membrane clusters. We also see in Fig. 3, that until here, a considerable drop of potential energy has occurred. During reorganisation of the lipid structures between (b) and (c), there is a steep gradient of $S_2(\tau)$ with another drops at ~200τ and ~250τ. These drops occur when the membranes iteratively fuse. Each time when merging occurs, $S_2(\tau)$ decreases, which indicates decreasing order in the system – then, when the number of separate membranes has been reduced and no merging process is going on anymore, $S_2(\tau)$ rises again, indicating the increased order as a result of membrane fusion. This process repeats itself several times as can be seen in Fig. 4, until finally only one merging process between the last two membranes remains. This membrane fusion occurs between (d) and (e), and after the last remaining membrane has reorganised itself, $S_2(\tau)$ has risen again and reached its largest value at (f), i.e. the order of the system has reached its maximum value at equilibrium. The iterative process of membrane fusion also results in a minimization of the energy, as indicated in Fig. 3.

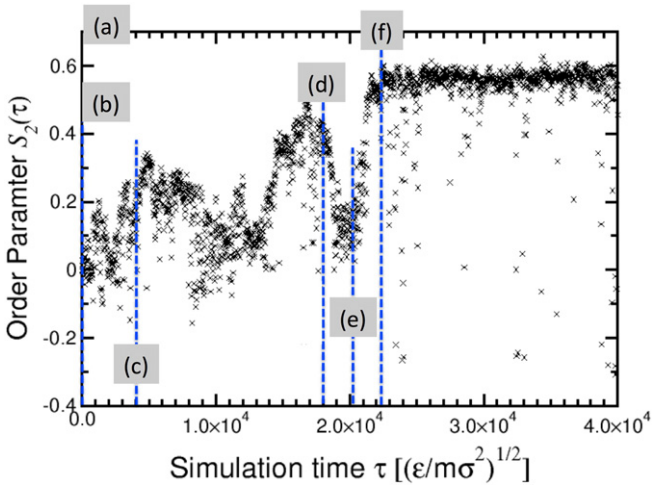

Fig. 4. Order parameter $S_2(\tau)$ vs. simulation time τ. The letters (a)–(f) correspond to different points in time corresponding to the snapshots in Fig. 2 and to the energy levels in Fig. 3. S_2 for (a) and (b) are actually close to zero and their boxes are just shifted for better visibility of the data.

3.2. Structural properties

3.2.1. Elastic modulus

The bending elasticity modulus κ_B determines by how much an applied external force deforms a lipid bilayer from its perfectly flat energetic ground state. It can be obtained from linear response theory by analyzing the bilayer height fluctuation spectrum. From Helfrich's linearized continuum theory [71] one can derive the following relation for a two-dimensional elastic sheet [17], [72]:

$$M(n) = \langle c_{\vec{n}}\, c_{\vec{n}}^{*} \rangle = \frac{k_B T L^2}{16\pi^4 \left(\kappa_B \vec{n}^{\,4} + s\vec{n}^{\,2}\right)}, \tag{8}$$

where

$$c_{\vec{n}} = \frac{1}{N}\sum_{j=1}^{N}(z_j - z_0)\ e^{\left[\frac{-2\pi i}{L}\left(n_x x_j + n_y y_j\right)\right]} \tag{9}$$

is a Fourier component of the deviation of the local bilayer height z_j with respect to its average height z_0. The sum in Eq. (9) runs over all bilayer particles with coordinates x_j, y_j, and z_j, where $\vec{n}$ is a two-dimensional vector with components n_x and n_y in reciprocal space, which relates to a wave-vector through

$$\vec{q} = \frac{2\pi\vec{n}}{L}. \tag{10}$$

The quantity s in Eq. (8) is the surface tension

$$s = L\left(2p_{zz} - p_{xx} - p_{yy}\right), \tag{11}$$

which is related to the diagonal components of the pressure tensor $p_{\alpha\beta}$. As we perform NPT MD simulations for the equilibrium properties, the pressure is isotropic with $p_{zz} = p_{xx} = p_{yy}$, i.e. the surface tension vanishes. Expressing Eq. (8) in terms of wave-vectors, we finally obtain for the regime of small wave vectors

$$M(q) \propto q^{-4}. \tag{12}$$

We simulate systems with 3000 lipids (i.e. $N = 9000$ lipid particles) and $L \approx 28$ nm, depending on the value of h_c. As shown in Fig. 5, the asymptotic q^{-4} scaling regime is recovered at this system size, which implies that the characteristic lipid bilayer bending modes can be accommodated with this size of the simulation box. We obtained the bending rigidities by fitting Eq. (8) to the simulation data. Continuum theory [17], [72] relates κ_B to the area compression modulus via

$$K_C = 24\kappa_B / d^2, \tag{13}$$

with d being the bilayer thickness, which we take to be 5 nm. Results of simulations for these quantities are provided in Table 1. The values obtained from our simulations for membranes in the fluid phase are well within the typical experimental range of these observables, which is $K_C \simeq 234$ mN/m, and $\kappa_B = 10 - 40\ k_BT$, depending on the technique used, such as micropipet aspiration or various forms of optical measurements [73], [74].

We note that our results for κ_B and K_C displayed in Table 1 are in better agreement with physiological data than was reported in several previous studies using coarse-grained numerical models [58], [60–62].

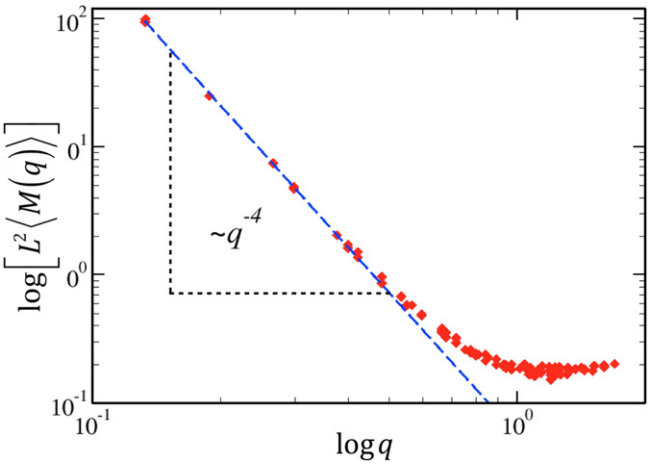

Fig. 5. Height fluctuation spectrum of a bilayer system with 3000 lipids and $h_c = 1\sigma$. The scaling of the spectrum follows the relation $M(q) \propto q^{-4}$ as predicted by scaling theory.

3.2.2. Pair correlation function

The local structure of the aggregated lipids is analyzed by the pair correlation function $g(r)$. As shown in Fig. 6, $g(r)$ exhibits distinct peaks indicating a very strong aggregation of the lipids for decreasing temperature T. For the lowest temperatures the system is practically frozen into a quasi-crystalline state showing long-range order even at distances beyond 5σ. With increasing temperature the system attains a different structure with only local order up to distances of roughly 3σ. Hence, in this range of temperature, the structural features of the aggregated lipids are similar to fluid behavior with fluctuations in the bilayer membrane height and shape. Finally, for very large temperatures, only the first and second nearest neighbor peaks remain which reflects in essence the local structure of single lipid molecules. This means that no aggregation of lipids occurs for this range of temperatures and the given value of h_c, and no bilayer membranes are formed.

3.2.3. Phase diagram

We have calculated a phase diagram of our lipid membrane model for a large range of temperature T and interaction parameter h_c. For this analysis we used systems with 1000 lipids at density $\rho = 0.05/\sigma^2$ in a cubic box length of $L \approx 39.15\ \sigma$. In Fig. 7 we can distinguish at least four different domains of system behavior:

In one domain, denoted with crosses in Fig. 7 no self-assembly of lipids occurs. Here, for a given attractive interaction range h_c of the lipid tails, the temperature and consequently, the thermal motion of the lipids is too large to allow for membrane formation.

Then there is a range of combinations of T and h_c where we observe formation of fluid membranes (denoted with filled circles in Fig. 7). The self-assembled membranes of this domain are the ones for which we have shown in our previous analysis that here we obtain values for the bending stiffness and the compression modulus which are within the range of typical experimental values for membranes in vivo and in vitro.

A third domain can be distinguished where clustering of lipids leads to stable bilayer membranes which have a solid-like local structure with long-range order as can be seen in the distinctive peaks of $g(r)$ in Fig. 6. This range in the phase diagram is denoted with dark squares in Fig. 7

Table 1
List of simulations of stable bilayers, performed for calculating the bending stiffness κ_B and the compression modulus K_C. Typical values of the lipid attraction parameter h_c are used. The simulation box size L is displayed as well.

h_c (σ)	L (nm)	κ_B (k_BT)	K_C ($\frac{\text{mN}}{\text{m}}$)
0.8	29.62 ± 0.01	13.4 ± 0.7	172 ± 6
1.0	29.27 ± 0.01	15.8 ± 0.8	192 ± 9
1.2	28.38 ± 0.01	17.9 ± 0.9	224 ± 15
1.4	27.16 ± 0.05	22.6 ± 1.1	240 ± 18

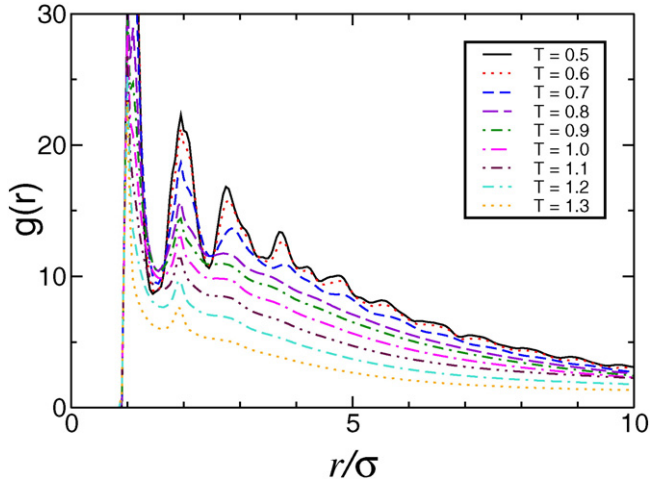

Fig. 6. Pair correlation function $g(r)$ for a system of 1000 lipids at density $\rho = 0.05/\sigma^3$ and degree of hydrophobicity $h_c = 1.3$ for different temperatures T in units of ε/k_B.

and leads to rather rigid bilayer structures exhibiting much less fluctuations in shape and height.

Finally, for larger values of both, h_c and T, we observe the formation of closed bilayer membrane vesicles within the fluid domain of the phase diagram, indicated in Fig. 7 with additional circles enclosing the data points. Each data point in Fig. 7 is obtained by analyzing at least five different realizations of fully equilibrated systems with the respective parameter pair (T, h_c) and simulation times of at least $10^5\tau$ after equilibration.

The sol-gel transition, as well as the transition between gel or fluid-like structural behavior of stable bilayer membranes and the domain where no structure formation occurs, can be distinguished rather unambiguously based on using a combination of evaluation methods: We use visual inspection of the simulated systems, the local structure obtained from the pair correlation function $g(r)$, and additionally the order parameter S_2. Whether or not closed bilayer vesicles in the lipid domain of the phase diagram are formed, additionally depends on the size of the simulated system, i.e. on the number of lipid molecules and on the size of the simulation box. Our box size is always chosen as a cube and is at least two times the size of the largest extension of the final lipid bilayer (either flat or in the form of a vesicle), thus avoiding any artificial stabilization effects.

Finally, in Fig. 8 we show for $T = 0.7\ \varepsilon/k_B$ the fluctuations of the order parameter $S_2(\tau)$ at equilibrium. One can clearly detect different average values of S_2 depending on the choice of h_c. The smallest value of S_2 for $h_c = 0.9$ for which no lipid assembly occurs (compare Fig. 7) is just above zero, the expected value for a complete random orientation of lipid molecules with no actual preferred direction. For values of $h_c \in [1.0, 1.2]$, we see increasing values of $S_2(\tau)$, indicating a preferred orientation of the average lipid direction. $h_c = 1.3$ is one of the very few limiting cases, where no definite conclusion can be drawn as to whether this data point still pertains to the fluid or the quasi-solid domain in Fig. 7. Neither a visual inspection of the systems, nor $g(r)$, along with $S_2(\tau)$ leads to a conclusive behavior, i.e. sometimes no clustering occurs, sometimes it does occur. Such ambiguous data points in the phase diagram are marked in Fig. 7 as a circle and a square. The largest values of h_c finally pertain to the quasi-solid domain which is consistent with these systems exhibiting the largest average values of S_2.

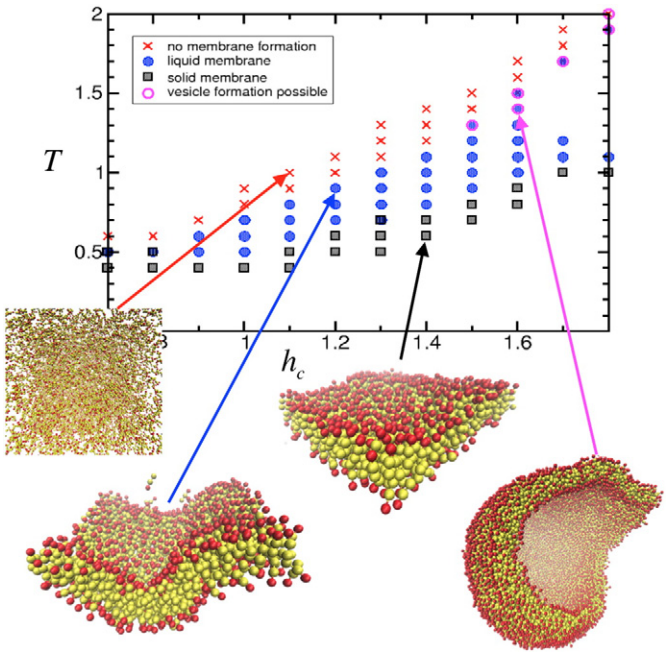

Fig. 7. Phase diagram of our membrane model with respect to temperature T and interaction parameter h_c. Four different phases can be distinguished: I. No clustering (crosses), II. A fluid, or gel-like phase where stable bilayer membranes are formed (circles). III. A quasi-crystalline phase where stable bilayers are formed with very small fluctuations in shape and membrane height (squares). IV. A fluid phase where closed bilayer membrane vesicles are formed (larger circles). Equilibrium simulation snapshots of typical structures of lipid molecules in the four different phases are displayed as well. Note the curved shape of the lipid membrane in the fluid phase and the more rigid structure in the quasi-crystalline phase.

4. Conclusions

We have presented molecular dynamics simulations of coarse-grained lipid molecules based on an extended standard polymer model with an additional interaction term mimicking hydrophobic behavior of lipid tails. While we are not limited with our model in the number of CG particles used for the head or tail part of the lipids, for the investigations presented here, we use a three-particle lipid version of our simulation model. The advantage of this model is that it is based on a well-tried CG model from computational polymer physics [25], [36], [39], [40]. It is also very flexible and allows for specifically tuning the properties of the resulting membranes. The model as we have presented it here is not adapted to any specific choice of lipids in contrast to the approaches in several previous numerical studies that investigated self-assembly of lipids, in particular when results were obtained using some standard software (e.g. Gromacs or AMBER) and the particular force fields provided by these software tools [14], [58], [59], [67], [68].

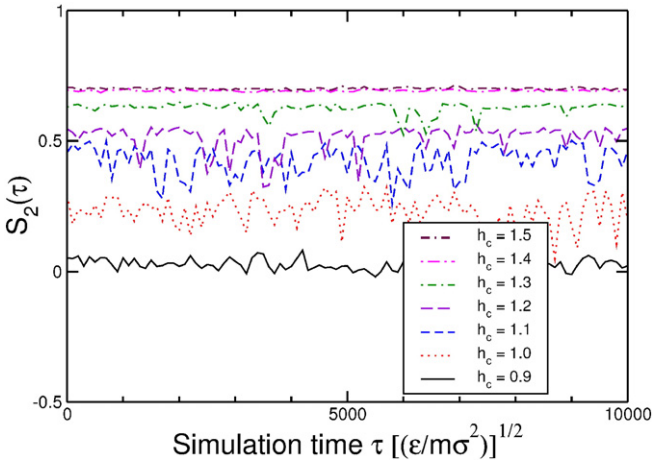

Fig. 8. Order parameter $S_2(\tau)$ according to Eq. (7) as a function of simulation time τ for $T = 0.7\ \varepsilon/k_B$ and different values of h_c.

We analyzed the dynamics of the lipid molecules when self-organizing into numerous, small clusters of lipid molecules, driven by the particular interaction potentials of our coarse-grained model that mimic the amphiphilic properties of phospholipid molecules. We observed several stages of clustering while the system approaches equilibrium and minimizes its total energy, until finally all individual clusters have merged into one stable structure. The most common stable structure produced with our model is a fluid (or gel-like) bilayer membrane, either with a flat shape or in closed form as a vesicle. For bilayer membranes at equilibrium we were able to show that with a proper choice of our model parameters we obtain values for the compression modulus and the bending stiffness within the range of typical experimental values.

We investigated the local structure of the bilayer membranes at equilibrium by means of the pair correlation function which shows sensitive dependence on the temperature with given lipid tail interaction range h_c and we introduced an order parameter based on the Legendre polynomials to further elucidate quantitatively the transition from a random initial state of unconnected lipid chains to highly ordered fluid phases or quasi-solid phases. Furthermore, we determined the parameter combinations for temperature T and lipid tail interaction h_c for the different phases, including a sol–gel transition and the occurrence of closed bilayer membrane vesicles. Finally, we presented results showing the dependence of the order parameter $S_2(\tau)$ of the membranes on the degree of hydrophobicity present in the system, and we discussed that the gradient of $S_2(\tau)$ seems to be a good indicator of major reorientations during self-assembly of lipids. We believe that in doing this, we have added several interesting new aspects in the discussion of the dynamics of lipid bilayer assembly in MD simulations based on CG models.

We plan to extend our model to topological variations of lipids with two and three tails and to perform systematic simulations with mixtures of these lipid variations. This will introduce interesting asymmetric effects into the self–assembly process that can be investigated systematically. Even more important, in follow-up applications of our model currently under way, we are investigating the effect of the interaction of shock waves with our bilayer membranes, in particular with vesicles, which may be used as simple mechanical models of the plasma membrane of eukaryotic cells. The larger context of this research program is the attempt to enhance our fundamental understanding of shock wave interaction with soft matter systems, in particular with cellular systems and biomolecules on a length scale comparable to the typical size of an eukaryotic cell. To the best of our knowledge, this idea of using *coarse-grained* particle models for soft matter systems in combination with the investigation of shock wave effects in these systems constitutes a fairly new approach.

Enhanced understanding of shock wave effects in soft biological matter could further enhance our understanding of tumor therapies in cancer research that are based on shock wave interaction with cancer tissue such as High Intensity Focused Ultrasound (HIFU), which has been used in clinical practice for many years, but which has not been well understood on a fundamental level.

Transparency Document

The Transparency document associated with this article can be found, in online version.

Acknowledgement

This work was supported financially by the Fraunhofer-Gesellschaft, e. V., Germany, under grant No. 600016, Vintage Class Program: “Shock Wave Induced Destruction of Tumor Cells”, and. “Extracorporeal, Focused Ultrasound Therapy: Effectiveness, Simulation, and Planning of New Therapies” under grant No 400017.

References

[1] D. Nelson, T. Piran, S. Weinberg (Eds.), Statistical Mechanics of Membranes and Interfaces, second ed.World Scientific Publishing Co., Inc, 2004.
[2] R. Phillips, J. Kondev, J. Theriot, Physical Biology of the Cell, first ed. Garland Science, Taylor and Francis Group, New York, 2009.
[3] B. Alberts, D. Bray, A. Johnson, J. Lewis, D. Morgan, M. Raff, K. Roberts, P. Walter, Molecular Biology of the Cell, fourth ed. Garland Science, Taylor and Francis Group, New York, 2000.
[4] S.J. Singer, G.L. Nicolson, The fluid mosaic model of the structure of cell membranes, Science 175 (1972) 720–731.
[5] H. Sprong, P. van der Sluijs, G. van Meer, How proteins move lipids and lipids move proteins, Nat. Rev. Mol. Cell Biol. 2 (2001) 504–513.
[6] G. van Meer, D.R. Voelker, G.W. Feigenson, Membrane lipids: where they are and how they behave, Nat. Rev. Mol. Cell Biol. 9 (2008) 112–124.
[7] M. Lindau, G. Alvarez de Toledo, The fusion pore, Biochim. Biophys. Acta 1641 (2003) 167–173.
[8] A. Mayer, Membrane Fusion in Eukaryotic Cells, Annu. Rev. Cell Dev. Biol. 18 (2002) 289–314.
[9] G. Brannigan, L.C.L. Lin, F.L.H. Brown, Implicit solvent simulation models for biomembranes, Eur. Biophys. J. 35 (2006) 104–124.
[10] P.J. Bond, J.M. Cuthbertson, S.S. Deol, M.S. Sansom, MD simulations of spontaneous membrane protein/detergent micelle formation, J. Am. Chem. Soc. 126 (2004) 15948–15949.
[11] P.J. Bond, M.S. Sansom, Insertion and assembly of membrane proteins via simulation, J. Am. Chem. Soc. 128 (2006) 2697–2704.
[12] R.O. Dror, M.O. Jensen, D.W. Borhani, D.E. Shaw, Perspectives on: molecular dynamics and computational methods: exploring atomic resolution physiology on a femtosecond to millisecond timescale using molecular dynamics simulations, J. Gen. Physiol. 135 (2010) 555–562.
[13] K. Lindorff-Larsen, S. Piana, K. Palmo, P. Maragakis, J.L. Klepeis, R.O. Dror, Perspectives on: molecular dynamics and computational methods: exploring atomic resolution physiology on a femtosecond to millisecond timescale using molecular dynamics simulations, Proteins 78 (2010) 1950–1958.
[14] A.A. Skjevik, B.D. Madej, C.J. Dickson, K. Teigen, R.C. Walker, I.R. Gould, All-atom lipid bilayer self-assembly with the AMBER and CHARMM lipid force fields, Chem. Commun. 51 (2015) 4402–4405.
[15] A.W. Götz, M.J. Williamson, D. Xu, D. Poole, S. Le Grand, R.C. Walker, Routine microsecond molecular dynamics simulations with AMBER on GPUs. 1. Generalized Born, J. Chem. Theory Comput. 8 (2012) 1542–1555.
[16] M. Orsi, J.W. Essex, Physical properties of mixed bilayers containing lamellar and nonlamellar lipids: insights from coarse-grain molecular dynamics simulations, emph-Faraday Discuss. 161 (2013) 249–272.
[17] R. Goetz, G. Gompper, R. Lipowsky, Mobility and elasticity of self-assembled membranes, Phys. Rev. Lett. 82 (1999) 221–224.
[18] S.O. Nielsen, C.F. Lopez, G. Srinivas, M.L. Klein, Topical review: coarse grain models and the computer simulation of soft materials, J. Phys. Condens. Matter 16 (2004) 481–R512.
[19] R. Lipowsky, Biomimetic membrane modelling: pictures from the twilight zone, Nat. Mater. 3 (2004) 589–591.
[20] A.P. Lyubartsev, Multiscale modeling of lipids and lipid bilayers, Eur. Biophys. J. 35 (2005) 53–61.
[21] Z.J. Wang, M. Deserno, A systematically coarse-grained solvent-free model for quantitative phospholipid bilayer simulations, J. Phys. Chem. B 114 (2010) 11207–11220.
[22] M.O. Steinhauser, Computational Multiscale Modeling of Fluids and Solids, first ed. Springer, Berlin, Heidelberg, New York, 2008.
[23] M. Orsi, J. Michel, J.W. Essex, Coarse-grain modelling of DMPC and DOPC lipid bilayers, J. Phys. Condens. Matter 22 (2010) 155106-1–155106-15.
[24] M. Müller, Studying amphiphilic self-assembly with soft coarse-grained models, J. Stat. Phys. 145 (2011) 967–1016.
[25] M.O. Steinhauser, in: L. Wang (Ed.), Molecular Dynamics - Studies of Synthetic and Biological Macromolecules, InTech 2012, pp. 1–28.
[26] V. Tozzini, Coarse-grained models for proteins, Curr. Opin. Struct. Biol. 15 (2004) 144–150.
[27] G.S. Ayton, W.G. Noid, G.A. Voth, Multiscale modeling of biomolecular systems: in serial and in parallel, Curr. Opin. Struct. Biol. 17 (2007) 192–198.
[28] P.P. Ghysels, G. Samaey, B. Tijskens, P. van Liedekerke, H. Ramon, D. Roose, Multi-scale simulation of plant tissue deformation using a model for individual cell mechanics, Phys. Biol. 6 (2008) 016009-1–016009-14.
[29] P. van Liedekerke, E. Tijskens, H. Ramon, P.P. Ghysels, G. Samaey, D. Roose, Particle-based model to simulate the micromechanics of biological cells, Phys. Rev. E 81 (2010) 061906-1–061906-15.
[30] M. Schmidt, U. Kahlert, J. Wessolleck, D. Maciaczyk, B. Merkt, J. Maciaczyk, J. Osterholz, G. Nikkhah, M.O. Steinhauser, Characterization of a setup to test the impact of high-amplitude pressure waves on living cells, Nat. Sci. Rep. 4 (2013) 3849.
[31] M.O. Steinhauser, M. Schmidt, Destruction of cancer cells by laser-induced shock waves: recent developments in experimental treatments and multiscale computer simulations, Soft Matter 10 (2014) 4778–4788.
[32] A. Warshel, M. Levitt, Theoretical studies of enzymic reactions: dielectric, electrostatic and steric stabilization of the carbonium ion in the reaction of lysozyme, J. Mol. Biol. 103 (1976) 227–249.
[33] R.G. Winkler, M.O. Steinhauser, P. Reineker, Complex formation in systems of oppositely charged polyelectrolytes: a molecular dynamics simulation study, Phys. Rev. E 66 (2002) 021802-1–021802-7.

[34] B. Dünweg, D. Reith, M.O. Steinhauser, K. Kremer, Corrections to scaling in the hydrodynamic properties of dilute polymer solutions, J. Chem. Phys. 117 (2002) 914–924.
[35] M.J. Stevens, Coarse-grained simulations of lipid bilayers, J. Chem. Phys. 121 (2004) 11942–11948.
[36] M.O. Steinhauser, A molecular dynamics study on universal properties of polymer chains in different solvent qualities. Part I. A review of linear chain properties, J. Chem. Phys. 122 (2005) 094901-1–094901-13.
[37] A.H. de Vries, A.E. Mark, S.J. Marrink, Molecular dynamics simulation of the spontaneous formation of a small DPPC vesicle in water in atomistic detail, J. Chem. Phys. 126 (2004) 4488–4489.
[38] M.O. Steinhauser, Computational methods in polymer physics, Recent Res. Dev. Phys. 7 (2006) 59–97.
[39] M.O. Steinhauser, K. Grass, E. Strassburger, A. Blumen, Impact failure of granular materials – Non-equilibrium multiscale simulations and high-speed experiments, Int. J. Plast. 25 (2008) 161–182.
[40] M.O. Steinhauser, J. Schneider, A. Blumen, Simulating dynamic crossover behavior of semiflexible linear polymers in solution and in the melt, J. Chem. Phys. 130 (2009) 164902-1–164902-8.
[41] M.G. Saunders, G.A. Voth, Coarse-graining methods for computational biology, Annu. Rev. Biophys. 42 (2012) 73–93.
[42] J.-M. Drouffe, A.C. Maggs, S. Leibler, S. Leibler, Computer simulations of self-assembled membranes, Science 254 (1991) 1353–1356.
[43] R. Goetz, R. Lipowsky, Computer simulations of bilayer membranes: self-assembly and interfacial tension, J. Chem. Phys. 108 (1998) 7397–7409.
[44] H. Noguchi, M. Takasu, Self-assembly of amphiphiles into vesicles: a brownian dynamics simulation, Phys. Rev. E 64 (2001) 041913-1–041913-7.
[45] G.K. Bourov, A. Bhattacharya, Brownian dynamics simulation study of self-assembly of amphiphiles with large hydrophilic heads, J. Chem. Phys. 122 (2005) 44702-1–44702-6.
[46] Z. Zhang, L. Lu, W.G. Noid, V. Krishna, J. Pfaendtner, G.A. Voth, A systematic methodology for defining coarse-grained sites in large biomolecules, Biophys. J. 95 (2008) 5073–5083.
[47] G.C. Ganzenmüller, S. Hiermaier, M.O. Steinhauser, Shock-wave induced damage in lipid bilayers: a dissipative particle dynamics simulation study, Soft Matter 7 (2011) 4307–4317.
[48] W.-X. Huang, C.B. Chang, H.J. Sung, Three-dimensional simulation of elastic capsules in shear flow by the penalty immersed boundary method, J. Comput. Phys. 231 (2012) 3340–3364.
[49] F.G. Pazzona, P. Demontis, G.B. Suffritti, A grand-canonical Monte Carlo study of the adsorption properties of argon confined in ZIF-8: local thermodynamic modeling, J. Phys. Chem. C 117 (2013) 349–357.
[50] S. Pogodin, V.A. Baulin, Coarse-grained models of phospholipid membranes within the single chain mean field theory, Soft Matter 6 (2010) 2216–2226.
[51] Y. Wang, J.K. Sigurdsson, E. Brandt, P.J. Atzberger, Dynamic implicit-solvent coarse-grained models of lipid bilayer membranes: fluctuating hydrodynamics thermostat, Phys. Rev. E 88 (2013) 023301-1–023301-5.
[52] G. Brannigan, F.L.H. Brown, Solvent-free simulations of fluid membrane bilayers, J. Chem. Phys. 120 (2004) 1059–1071.
[53] G. Brannigan, P.F. Philips, F.L.H. Brown, Flexible lipid bilayers in implicit solvent, Phys. Rev. E 72 (2005) 011915-1–011915-4.
[54] O. Farago, "Water-free" computer model for fluid bilayer membranes, J. Chem. Phys. 119 (2003) 596–605.
[55] Z.-J. Wang, D. Frenkel, Modeling flexible amphiphilic bilayers: a solvent-free off-lattice Monte Carlo study, J. Chem. Phys. 122 (2005) 234711.
[56] J.D. Revalee, M. Laradji, P.B. Sunil Kumar, Implicit-solvent mesoscale model based on soft-core potentials for self-assembled lipid membranes, J. Chem. Phys. 128 (2008) 035102–035109.
[57] A.J. Sodt, T. Head-Gordon, An implicit solvent coarse-grained lipid model with correct stress profile, J. Chem. Phys. 132 (2010) 205103.
[58] S.J. Marrink, A.H. de Vries, A.E. Mark, Coarse grained model for semiquantitative lipid simulations, J. Phys. Chem. B 108 (2003) 750–760.
[59] A.Y. Shih, A. Arkhipov, P.L. Freddolino, K. Schulten, Coarse grained protein-lipid model with application to lipoprotein particles, J. Phys. Chem. B 110 (2006) 3674–3684.
[60] H. Noguchi, Solvent-free coarse-grained lipid model for large-scale simulations, J. Chem. Phys. 134 (2011) 055101.
[61] I.R. Cooke, K. Kremer, M. Deserno, Tunable generic model for fluid bilayer membranes, Phys. Rev. E 72 (2005) 011506-1–011506-4.
[62] M.-J. Huang, R. Kapral, A.S. Mikhailov, H.-Y. Chen, Coarse-grain model for lipid bilayer self-assembly and dynamics: multiparticle collision description of the solvent, J. Chem. Phys. 137 (2012) 055101-1–055101-10.
[63] H. Noguchi, M. Takasu, Adhesion of nanoparticles to vesicles: a brownian dynamics simulation, Biophys. J. 83 (2002) 299–308.
[64] I.R. Cooke, M. Deserno, Solvent-free model for self-assembling fluid bilayer membranes: Stabilization of the fluid phase based on broad attractive tail potentials, J. Chem. Phys. 123 (2005) 224710-1–224710-13.
[65] S. Izvekov, G.A. Voth, Solvent-free lipid bilayer model using multiscale coarse-graining, J. Phys. Chem. B 113 (2009) 4443–4455.
[66] H. Yuan, C. Huang, J. Li, G. Lykotrafitis, S. Zhang, One-particle-thick, solvent-free, coarse-grained model for biological and biomimetic fluid membranes, Phys. Rev. E 82 (2010) 011905.
[67] J.C. Shelley, M.Y. Shelley, R.C. Reeder, S. Bandyopadhyay, M.L. Klein, A coarse grain model for phospholipid simulations, J. Phys. Chem. B 105 (2001) 4464–4470.
[68] J.C. Shelley, M.Y. Shelley, R.C. Reeder, S. Bandyopadhyay, P.B. Moore, M.L. Klein, Simulations of phospholipids using a coarse grain model, J. Phys. Chem. B 105 (2001) 9785–9792.
[69] M.O. Steinhauser, Static and dynamic scaling of semiflexible polymer chains—a molecular dynamics simulation study of single chains and melts, Mech. Time-Depend. Mater. 12 (2008) 291–312.
[70] H.J.C. Berendsen, J.P.M. Postma, W.F. van Gunsteren, A. DiNola, J.R. Haak, Molecular dynamics with coupling to an external bath, J. Chem. Phys. 81 (1984) 3684–3698.
[71] W. Helfrich, Elastic properties of lipid bilayers: theory and possible experiments, Z. Naturforsch. C 28 (1973) 693–703.
[72] U. Seifert, Configurations of fluid membranes and vesicles, Adv. Phys. 46 (1997) 13–137.
[73] K. Olbrich, W. Rawicz, D. Needham, E. Evans, Water permeability and mechanical strength of polyunsaturated lipid bilayers, Biophys. J. 79 (2000) 321–327.
[74] C.-H. Lee, W.-C. Lin, J. Wang, All-optical measurements of the bending rigidity of lipid-vesicle membranes across structural phase transitions, Phys. Rev. E 64 (2001) 020901-1.